Rare Met. (2022) 41(7):2200–2216
https://doi.org/10.1007/s12598-021-01908-9

RARE METALS

MINI REVIEW

Generation and manipulation of skyrmions and other topological spin structures with rare metals

Chu Ye, Lin-Lin Li, Yun Shu, Qian-Rui Li, Jing Xia, Zhi-Peng Hou, Yan Zhou, Xiao-Xi Liu, Yun-You Yang, Guo-Ping Zhao*

Received: 31 August 2021 / Revised: 3 October 2021 / Accepted: 12 October 2021 / Published online: 2 February 2022

Abstract Skyrmions are nano-scale quasi-particles with topological protection, which have potential applications in next-generation spintronics-based information storage. Numerous papers have been published to review various aspects of skyrmions, including physics, materials and applications. However, no review paper has focused on rare metals which play important roles in nucleating and manipulating skyrmions and other topological states. In this paper, various roles of rare metals have been classified and summarized, which can tune Curie temperature (T_C), Dzyaloshinskii–Moriya interaction (DMI), magnetocrystalline anisotropy, Ruderman–Kittel–Kasuya–Yosida (RKKY) interaction and four-spin interaction so as to trigger the generation of skyrmions and other topological spin structures. The materials covered include typical B20 crystals, various layered systems with interfacial DMI, frustrated materials, antiferromagnets, ferrimagnets, two-dimensional (2D) materials, etc. In addition, the rare-earth (RE) permanent magnets can provide an energy barrier and enrich the dynamic behaviors of skyrmions, which has also been reviewed.

Keywords Magnetic skyrmions; Rare metals; Generation and manipulation

Chu Ye and Lin-lin Li have contributed equally to this work.

C. Ye, L.-L. Li, Y. Shu, Q.-R. Li, J. Xia, Y.-Y. Yang, G.-P. Zhao*
College of Physics and Electronic Engineering, Sichuan Normal University, Chengdu 610068, China
e-mail: zhaogp@uestc.edu.cn

J. Xia, G.-P. Zhao
Center for Magnetism and Spintronics, Sichuan Normal University, Chengdu 610068, China

Z.-P. Hou
Guangdong Provincial Key Laboratory of Optical Information Materials and Technology, Guangzhou 510006, China

Z.-P. Hou
Institute for Advanced Materials, South China Normal University, South China Academy of Advanced Optoeletronics, Guangzhou 510006, China

Y. Zhou
School of Science and Engineering, The Chinese University of Hong Kong, Shenzhen 518172, China

X.-X. Liu
Department of Electrical and Computer Engineering, Shinshu University, Nagano 380-8553, Japan

1 Introduction

Skyrmions are topologically protected quasi-particles, which were proposed in nuclear physics by Skyrme in 1962 [1] and theoretically predicted to be stable in magnets by Bongdnov and Yablonskii [2] in 1989. The first experimental observation of skyrmions was carried out in MnSi, using the neutron scattering method by Pfleiderer's group at Technische Universität München from Germany [3]. These exotic spin structures were then successfully observed in real space using Lorentz image, in other B20-type materials, including $Fe_{0.5}Co_{0.5}Si$ [4, 5], MnGe [6] and FeGe [7] etc. Later, room-temperature skyrmions were found to exist stably in thin films [8–13] and multilayers [14–19] composed of alternating heavy metals and magnetic layers, which can be driven by the spin current readily.

Recently, robust skyrmions have been found in synthetic antiferromagnets [20–22], where the skyrmion Hall effect (SkHE) can be offset and hence skyrmions can be used in racetrack memory without the danger of losing the signal. Various types of skyrmions are also observed in ferrimagnets [23], ferroelectrics [24–26], antiferromagnets [27], semiconductors [28], superconductors [29] and two-dimensional (2D) materials [30–32]. In the meantime, other topological spin structures, such as antiskyrmions [33–36], bimerons [37], skyrmioniums [38], vortices [39, 40], half skyrmions [41], hopfions [42] and skyrmion bundles [43], have been investigated extensively in various materials. Skyrmions-related literatures have increased exponentially in recent years, and more than 400 papers were published in 2020, as given by Web of Science and shown in Fig. 1.

Up to now, there are more than 60 skyrmions-related review articles have been published, most of which review one aspect of the skyrmions classified according to the physics, the materials or the applications [44–55]. However, few review articles focus on the role of rare metals so far, which play important roles in nucleating and controlling skyrmions as well as other topological spin structures. In this paper, we will systematically summarize the role of rare metals in generating and manipulating skyrmions and other topological spins, including rare-dispersed metals Ga, Ge, etc., and the noble metals Pt and rare-earth (RE) metals Nd etc.

2 Role of rare metals in generating skyrmions in B20 and other non-centrosymmetric materials

Magnetic skyrmions were first reported in 2009 by Mühlbauer et al. [3], which were found via the small-angle neutron scattering (SANS) method in a B20-type material, MnSi. As shown in Fig. 2a, the skyrmion in MnSi can only occur at very low temperatures (below 30 K), which, however, aroused great interests immediately due to its potential application in spintronics. Yu et al. [4] observed real-space skyrmions in $Fe_{1-x}Co_xSi$, another B20 material, based on Lorentz transmission electron microscopy (LTEM), as shown in Fig. 3a [5], which can only appear in a narrow temperature region from 7 to 36 K.

High-temperature skyrmions are found later in MnGe [6], FeGe [7] and other B20 materials with rare metals, which can exist at the zero magnetic field and are stable in a wider temperature range. Spontaneous ground-state skyrmions in MnGe can be stabilized up to 150 K, which is near its Curie temperature (T_C = 170 K), as shown in Fig. 2b [5]. In the meantime, stable skyrmions are found in the FeGe thin-film from 50 K to the room temperature, as shown in Fig. 3b [5], due to its high Curie temperature (T_C = 280 K). Recently, the so-called three-dimensional (3D) skyrmion, i.e., the skyrmion bundle, containing the skyrmion bag and ending with the chiral vortex, has also been obtained in the FeGe thin film [45]. Other B20 materials, such as $Mn_{1-x}Fe_xSi$ [56] and $Mn_{1-x}Fe_xGe$ [57], can host skyrmions as well, with skyrmions in $Mn_{1-x}Fe_xGe$ being stable at a much higher temperature than those in $Mn_{1-x}Fe_xSi$.

As demonstrated above, the existence of Ge, a typical rare-dispersed metal, in various B20 chiral magnetic materials can help to stabilize skyrmions in a wider temperature range. Ge can induce strong spin–orbit coupling (SOC) to enhance DMI, which competes with the ferromagnetic exchange interaction to induce the peculiar twists of the spins and hence the formation of the skyrmions [6, 7, 57]. Later, it is found that other rare metal elements,

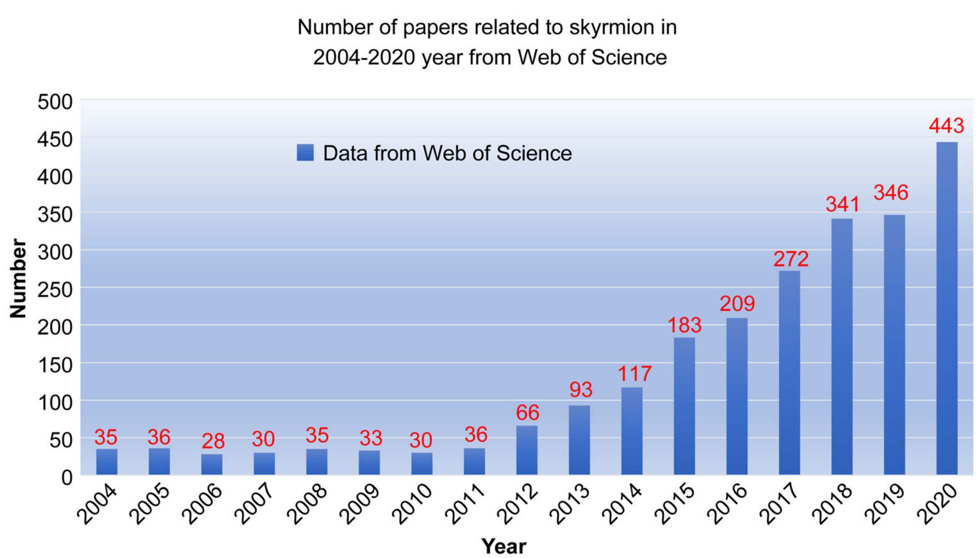

Fig. 1 Number of papers related to skyrmion in the year of 2004–2020 from Web of Science

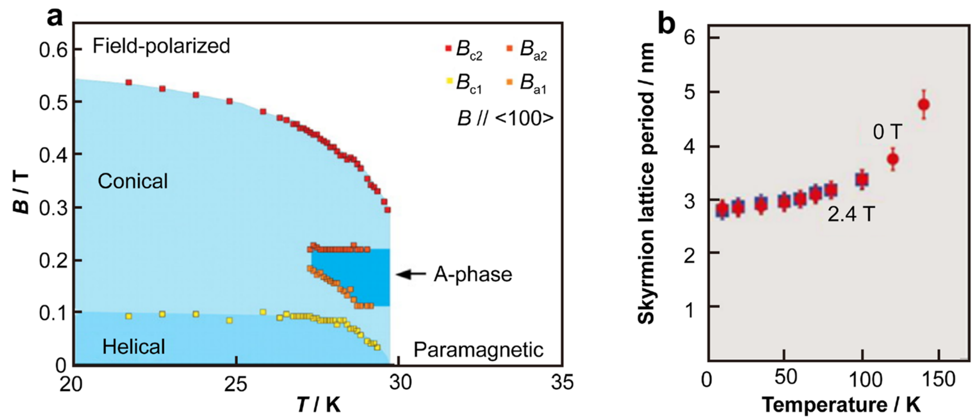

Fig. 2 Comparison of phase diagrams of MnSi and MnGe, indicating role of rare metal Ge in stabilizing skyrmions. **a** *B-T* phase diagram of MnSi, where skyrmions (A-phase) can only exist in a narrow temperature range of 28–30 K. Reproduced with permission from Ref. [5]. Copyright 2018, Institute of Physics Publishing. **b** Change of skL period in MnGe with temperature at different applied fields, indicating that skyrmions can be stable in a wide temperature range of 10–150 K. Reproduced with permission from Ref. [6]. Copyright 2015, American Chemical Society

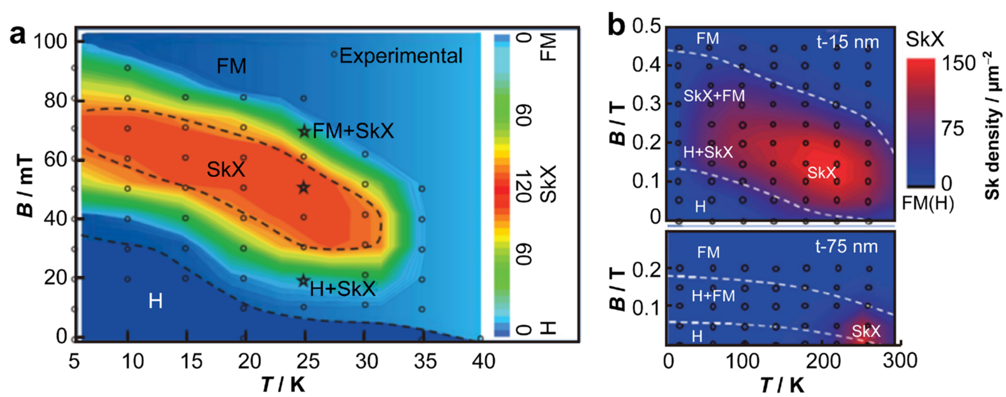

Fig. 3 Comparison of phase diagrams of $Fe_{0.5}Co_{0.5}Si$ and FeGe, indicating role of rare metal Ge in stabilizing skyrmions. **a** Phase diagrams of spin textures observed in a thin film of $Fe_{0.5}Co_{0.5}Si$ using Lorentz TEM, where skyrmions can only occur below 30 K; **b** phase diagrams for FeGe thin films with various values of thickness, demonstrating that skyrmions are stable from 50 K to room temperature. Reproduced with permission from Ref. [5]. Copyright 2018, Institute of Physics Publishing

including Se, Mo and Rh, can also increase the critical temperature and enhance the stability of the hosted skyrmions [58–60].

Skyrmions can occur in GaV_4S_8, a typical semiconductor material, in a narrow temperature range of 9–13 K [28], while they can be observed from 0 to 18 K in GaV_4Se_8 [58, 61]. Similarly, the transition temperature in the ferroelectric material $GaMo_4S_8$ is only 17.5 K, which can be raised to 27.5 K in $GaMo_4Se_8$ [59]. These results demonstrate that the rare metal Se can also improve SOC, enhance the DMI and help to stabilize skyrmions. Later, it is found that the incorporation of rare metal Rh into the strong ferromagnetic material Fe_2Mo_3N can produce significant DMI and stabilize skyrmions [60].

As summarized in Table 1, B20 materials with rare metals Ge, MnGe, FeGe and $Mn_{1-x}Fe_xGe$ [5–7, 57, 62] have much higher T_C than their counterparts without rare metals, indicating the important role of rare metal Ge in stabilizing skyrmions in these materials. At the same time, the substitution of Se in GaV_4S_8 and $GaMo_4S_8$ and incorporation of Rh into Fe_2Mo_3N can increase T_C and produce large DMI as well [22, 28, 58–60, 63].

3 Role of rare metals in layered systems with interfacial DMI

As demonstrated above, the DMI plays a key role in the generation of skyrmions, which occurs not only in systems with broken central symmetry, but also at the interface between ferromagnetic and heavy metals. As early as 1990, Fert [64] predicted the possibility of interfacial DMI in such thin film structures. The presence of skyrmion is stabilized by DMI provided by strong SOC at the interface

Table 1 Comparison of properties for typical non-centrosymmetric magnetic materials to demonstrate roles of rare metals in generating and stabilizing skyrmions

Materials	Point group	T_C/K	Skyrmion	Conductivity	Refs.
MnSi	T	30	2D, Bloch	Metal	[3]
MnGe	T	170	3D, Hedgehog	Semiconductor	[6]
$Fe_{1-x}Co_xSi$	T	7–36	2D, Bloch	Semiconductor	[4]
FeGe	T	278	2D, Bloch	Metal	[7]
$Mn_{1-x}Fe_xSi$	T	6.8–16.5	2D, Bloch	Metal	[56]
$Mn_{1-x}Fe_xGe$	T	150–220	2D, Bloch	Metal	[57]
GaV_4S_8	C_{3V}	13	2D, Néel	Semiconductor	[28]
GaV_4Se_8	C_{3V}	18	2D, Néel	Insulator	[58]
$GaMo_4S_8$	C_{3V}	17.5	2D, Néel	Insulator	[24]
$GaMo_4Se_8$	C_{3V}	27.5	2D, Néel	Insulator	[59]
$FeCo_{0.5}Rh_{0.5}Mo_3N$	O	132	2D, Bloch	Metal	[60]

of the heavy metal layer and perpendicular magnetic anisotropy (PMA) in the ferromagnetic layer [64–66], as shown in Fig. 4a for Co/Pt thin films [8].

At the Co/Pt interface, due to the strong SOC in the rare metal (Pt) and the broken mirror symmetry of the magnetic material thin film (Co), an indirect exchange interaction conducted by the rare metal atoms will occur between two nearby magnetic atoms in the system [8, 9, 16–18, 67]. The symmetry of DMI at the interface in the magnetic film systems containing heavy metals is different from that in the B20 structure system. As shown in Fig. 4b, the interfacial DMI in the magnetic film system yields Néel-type skyrmions [28], whereas skyrmions induced by DMI in the B20 system are usually Bloch-type, as shown in Fig. 4c [5]. The rare metal Pt in the Co/Pt layered system provides both strong SOC and large PMA, which are both necessary for the formation of skyrmions in thin-film systems.

Néel-type skyrmion was also found in monolayer Fe/Ir [68], where the heavy metal Ir offers strong SOC and hence the large interfacial DMI. In addition to the interfacial DMI, the four-spin interaction in the system competes with the Heisenberg exchange interaction to form a Néel-type skyrmion with a diameter of only 1 nm, as shown in Fig. 4, which is the smallest skyrmion found in experiments up to now [69–72]. In this case, the rare metal Ir provides both the large SOC and the nontrivial four-spin interaction, which are responsible for the occurrence of the atomic level skyrmions.

The above thin-film systems, offering strong SOC and DMI, have been extended to multilayer structures composed of magnetic and heavy metals alternatively. The control of interfacial DMI and PMA in such materials can be achieved by changing the thickness, material combination and other parameters of magnetic film and rare metal film [14, 19, 73–78], which gives the material system a

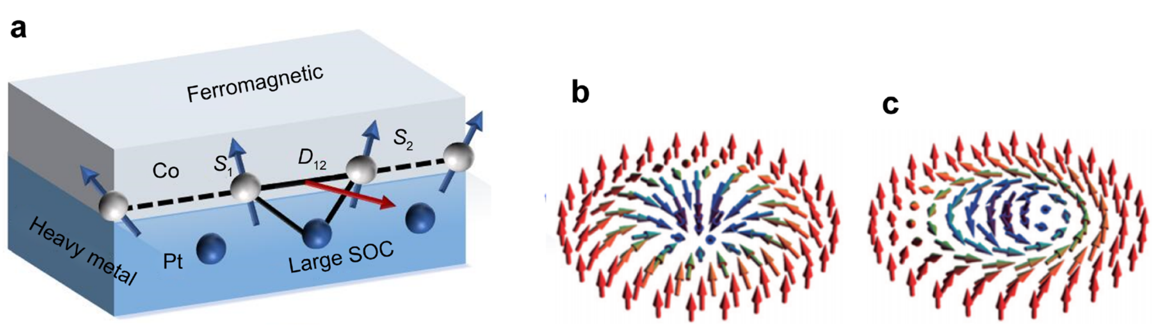

Fig. 4 DMI in Co/Pt layered system, which helps to produce Néel-type skyrmions. **a** Sketch of a DMI at interface between a ferromagnetic metal (grey) and a rare metal (heavy metal) with a strong SOC (blue), where DMI vector D_{12} related to triangle composed of two magnetic sites and an atom with a large SOC is perpendicular to plane of triangle. Because a large SOC exists only in the bottom metal layer, this DMI is not compensated by a DMI coming from a symmetric triangle. **b** Néel-type skyrmion induced by DMI illustrated in **a**, where in-plane spins orient in radius direction; **c** in contrast, Bloch-type skyrmion usually occurring in B20 crystals is vortex like, where in-plane spins are circling around center. Reproduced with permission from Ref. [5]. Copyright 2018, Institute of Physics Publishing

great degree of freedom, reduces skyrmion size and optimizes the stability and dynamic properties of skyrmions [79]. Two typical multilayers, $[Ir/Co/Pt]_{10}$ [14] and $[Pt/Co/Ta]_{15}$ [15], have been used in experiments to generate skyrmions. First-principles calculations show that the chiral direction of DMI provided by the two rare metals is opposite in the separate Ir/Co (Ta/Co) and Pt/Co structures, which, interestingly, can enhance the strength of DMI and facilitate the nucleation of the skyrmions [79, 80].

Quite a few experiments [81, 82] and calculations [18, 83, 84] show that the magnetic chirality at the Ir/Co interface is opposite to the Pt/Co interface, where large DMI has been observed in some Pt/Co/Ir multilayers. However, experiments using magnetic domain walls indicated that the magnetic chirality of the Ir/Co interface is the same as that of the Pt/Co interface [85, 86]. Further experiments confirm that the effective spin Hall angle of Ir has the same sign as Pt, suggesting that the sign of the DM exchange constant for Pt/Co and Ir/Co interfaces is the same, leading to a reduced DMI in some Pt/Co/Ir multilayers [87]. The DMI at the Ir/Co interface thus seems to depend on factors that are yet to be determined.

Recently, 3D spin configurations have been observed in $[Ir/Co/Pt]_N$ multilayers shaped into nanoscale disks where the skyrmion tube or the Hopfion is created [42]. With substantial DMI and PMA induced by the rare metals Ir and Pt into Co, these spin textures have a robust 3D structure [42].

Skyrmions are also found in layered metal/oxide heterostructures [19, 75], where the typical material is Ta/CoFeB/TaO_x multilayers. First-principles calculations indicate that the interfacial DMI can originate not only from the interface between rare metal Ta and the ferromagnetic layer but also from the interface between rare metal oxide TaO_x and the ferromagnetic layer [75]. First-principles calculations also demonstrate that the interfacial DMI between the ferromagnetic layer and rare metal oxide is related to charge transfer and electric polarization at the interface [75]. In this situation, rare metal oxides can increase the strength of DMI, thereby reducing the skyrmion size and improving the stability of skyrmions.

Another layered system proposed to generate skyrmions is the synthetic AFM multilayer structure based on rare metals, which has the advantage of inhibiting the SkHE and hence avoiding signal loss [20]. As shown in Fig. 5, there is strong AFM exchange coupling between two skyrmions with opposite polarity so that the net Magnus force is 0 and the SkHE is completely suppressed. Skyrmions have been successfully generated in various synthetic AFM multilayers, including [Co/Pd]/Ru/[Co/Pd] and $[Co/Pt]_N$/NiO/$[Co/Pt]_N$ multilayers [21, 22]. The rare metals Pd and Pt here are to provide strong DMI, which is necessary for the formation of Néel-type skyrmions. On the other hand, the rare metal Ru is to enable the AFM exchange coupling between the upper and the lower Co/Pd layers and hence to suppress the SkHE, similar to the role of NiO in $[Co/Pt]_N$/NiO/$[Co/Pt]_N$.

4 Role of rare metals in manipulating skyrmions and other spin textures in layered systems

As mentioned in the last section, the synthetic AFM multilayer has been proposed as an ideal structure to overcome skyrmion Hall effect, where a pair of skyrmions with opposite polarity driven by the electric current can move along the racetrack without any transverse drift. Such spin-polarized electric current can be applied in various layered systems, with spin orbit torques [11, 88] or spin transfer torques [89] induced in the magnetic layers to direct the motion of skyrmions. In particular, there have been many researches on control of skyrmions by SOT at room temperature, with rare metals as an important host for the electric current. For example, Néel-type skyrmions have been created in Ta/$Co_{20}Fe_{60}B_{20}$ (CoFeB)/MgO system by inserting an ultrathin Ta layer between the CoFeB and MgO [11], where skyrmions can be driven along racetracks by the SOT. The interfacial DMI due to the adjacent Ta rare metal layer with a large spin–orbit coupling facilitates the formation of the Néel-type skyrmions.

Further, SOT in various kinds of AFM/FM exchange bias has been used to generate and manipulate skyrmions [13]. Skyrmions can be created at the zero-field due to the exchange bias at the IrMn/CoFeB interface in Ta/$Ir_{22}Mn_{78}$/$Co_{20}Fe_{60}B_{20}$/MgO/Ta system [13], where spins in antiferromagnetic IrMn have a sizable spin Hall angle, allowing SOT to control skyrmions. The rare metal Ir is responsible for the antiferromagnetic order in IrMn and hence for the formation of exchange bias in the system, in addition to the large interfacial DMI of the system.

Compared to the normal FM/HM system [10], the IrMn/CoFeB heterostructure has displayed some unique advantages in generating and tuning skyrmions. First, the exchange bias at the IrMn/CoFeB interface can eliminate the need for an external magnetic field, leading to zero-field skyrmion formation. Second, the antiferromagnetic order and PMA can be tuned by the IrMn and CoFeB film thicknesses, lending additional flexibility in interfacial control. Third, a sizable SOT in the IrMn permits energy-efficient current control of skyrmions. The rare metals Ta and Ir work together to provide exchange bias, adjust PMA and enhance DMI, so that a single skyrmion can be generated and tuned at the room-temperature and the zero field.

For a dynamic skyrmion in the racetrack, the local exchange-bias field (LEBF) [90–92] generated by the

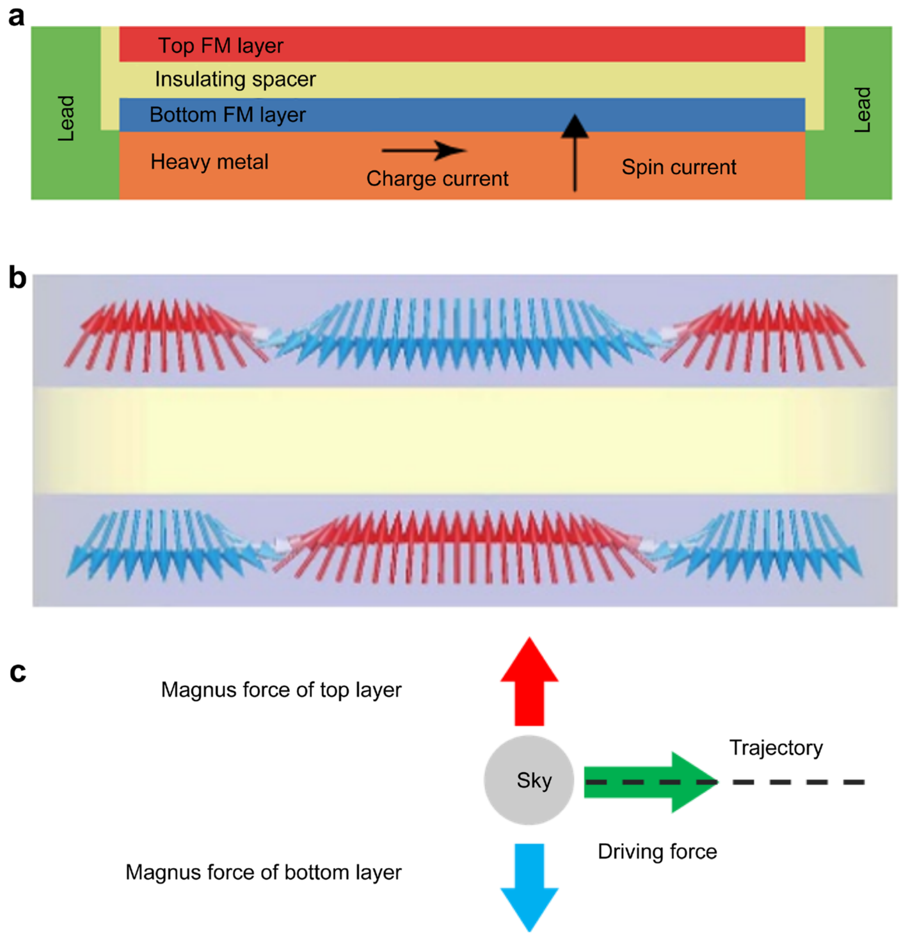

Fig. 5 Skyrmions in synthetic antiferromagnetic (AFM) multilayer, where Magnus force is 0. **a** AFM-coupled bilayer nanotrack for study of motion of a bilayer-skyrmion driven by current perpendicular to plane, where charge current flows through heavy-metal substrate along *x*-direction, which gives rise to a spin current ($p = +y$) perpendicularly injected to bottom ferrimagnetic layer because of spin Hall effect; skyrmion in bottom ferrimagnetic layer is driven by spin current, whereas skyrmion in top ferrimagnetic layer moves accordingly due to interlayer AFM exchange coupling. **b** Side view of bilayer-skyrmion. Reproduced with permission Ref. [20]. Copyright 2016, Springer Nature. **c** Schematic diagram of force analysis in synthetic AFM multilayers, where Magnus forces in top and bottom layers cancel each other so that skyrmion moves in the direction of the driving current without drift

IrMn/CoFeB interface can be used to suppress SkHE effectively. The pinning effect by LEBF can make the skyrmion move along the current direction when it is driven by the pulsed current. Here, the rare metal Ir can enhance DMI and stabilize skyrmions in the racetrack. Most importantly, Ir helps to provide the LEBF in IrMn/CoFeB system, which supply an energy barrier and prevent the skyrmion from annihilating at the racetrack edge [12].

Besides synthetic AFM and exchanging bias, there are other methods to overcome SkHE, which can cause the disastrous loss of skyrmion signal. Rare-earth permanent magnets can provide additional energy barrier, similar to the LEBF, which will be discussed in Sect. 6. On the other hand, the Magnus force in the AFM materials is cancelled due to two sets of antiferromagnetic coupled sublattice, which is similar to the case in synthetic AFM and will be elaborated in Sect. 7. In addition, various other potential barriers have been proposed to confine skyrmions in the center region of the racetrack so that the annihilation at the racetrack edge is avoided [93–98]. Generally, the rare metals can offer tunnelable PMA as well as DMI and hence the necessary energy barriers, in addition to large SOT under the aid of the electric current.

As displayed above, the spin-polarized current provides an electric method to manipulate skyrmions, which has been used extensively in both experiments and simulations. This method, however, results in undesired Joule heating effects, so that other methods have been proposed to control skyrmions, including magnetic field [89, 99], magnetic field gradient [100], spin wave [101–103] and thermal gradient [104]. It should be noted that these methods together with the spin-polarized current can manipulate other exotic topological spin textures, e.g., skyrmionium [103], bimeron [99], bimeronium [95] and antiskyrmion

[89]. In any case, rare metals can provide large DMI and PMA to realize the ideal motion of skyrmions and other spin textures.

Recently, various simulations [105] have shown that the electrical field can help to reverse the magnetic moments and hence to manipulate skyrmions in Cu_2OSeO_3 single crystal sample [106, 107] and CoFeB-MgO nanodisks [108], where the role of rare metals is not identified clearly. Generally, the rare metal can provide large enough DMI and facilitate the formation of skyrmions.

Later in 2019, Ma et al. [109] successfully generated and guided skyrmion bubbles in a [Pt(0.5 nm)/CoNi(0.5 nm)/Pt(0.5 nm)/CoNi(0.5 nm)/Pt(1 nm)] multilayer racetrack at room temperature, where the PMA could be finely tuned by the electric field in both the experiment and the simulation. The rare metal Pt helps to provide adjustable DMI and PMA through the change of the layer thickness, leading to the electric-field induced creation and directional motion of topological spin textures. In the experiment, the multilayer is sandwiched between the indium tin oxide/dielectric bilayer and the glass substrate, resulting in rare metal (Pt)/dielectric (SiO_2) interfaces. Importantly, the large anisotropy change can be produced in the interfaces with electric quadrupole induction, which is different from the normal ferromagnet/dielectric interface. The mechanism of generating and manipulating skyrmions and other spin textures in some special materials (frustrated material and so on) will be discussed in next sections.

5 Role of rare metals in generating skyrmions in other materials

5.1 Role of rare metals in frustrated materials

Skyrmions have also been found in materials without DMI, particularly in frustrated materials, where competing exchange interactions or generalized RKKY interactions are responsible for the appearance of chiral spin structures. Skyrmion lattices (skLs) have been identified at low temperatures in gadolinium compounds $GdRu_2Si_2$ [110], Gd_2PdSi_3 [111] and $Gd_3Ru_4Al_{12}$ [112], with the corresponding phase diagrams shown in Fig. 6. The formation of skLs is mainly due to the RKKY interactions in these materials, i.e., the coupling between the itinerant electrons and the local magnetic moments. Most itinerant electrons come from the 4d orbit of Ru, while the local magnetic moments result from the 4f orbit of Gd. Here, the rare metals, Gd and Ru, play important roles in providing the frustration and hence the formation of skLs. Chiral spin structures have also been found in other frustrated materials. Notably, Hou et al. [113–116] found high-temperature skyrmion bubbles in Fe_3Sn_2 and conducted a series of studies on their generation and manipulation.

Zhang et al. systematically studied the static and dynamic properties of skyrmions and other topological spin structures in the frustrated material, including bimerons [37], bimeronium [117] and skyrmionium [38]. Using micromagnetic modeling, they found that $Pb_2VO(PO_4)_2$ could be a suitable frustrated material for hosting skyrmions, where the frustration comes from the competition between the small nearest neighbor ferrimagnetic interaction and the large next-nearest neighbor AFM interaction. The AFM interaction originates from the rare metal V through the bridge of two oxygen atoms [118].

5.2 Role of rare metals in other centrosymmetric materials

It is noted that skyrmions and other topological spin structures have also been reported in other centrosymmetric materials. Biskyrmions have been identified in $La_{2-2x}Sr_{1+2x}Mn_2O_7$ [119] and MnNiGa [120–122], while skyrmion bubbles and skyrmions have also been found in $La_{1-x}Sr_xMnO_3$ [123] and $BaFe_{12-x-0.05}Sc_xMg_{0.05}O_{19}$ (BFSO) [124], respectively. Here, the RE metals La and Ga are to provide and adjust the magnetic moments of the materials, while the doping of the rare metal Sc in BFSO film is mainly to tune the magnetic crystalline anisotropy [124].

5.3 Role of rare metals in 2D van der Waals and ferroelectric materials

Recently, 2D van der Waals (vdW) materials are also reported to be a suitable material for hosting topological spin structures. Particularly, Bloch-type skyrmion bubbles and Néel-type skyrmions have been found in single crystals of 2D vdW material Fe_3GeTe_2 [30] and 2D vdW heterostructure WTe_2/Fe_3GeTe_2 [31], respectively. Both layers in the heterostructure have rare metal Te atoms, whose coupling enhances the DMI of the system and helps to form skyrmions [31]. Furthermore, the dynamics of the bimerons generated in the 2D vdW multiferroic heterostructure $LaCl/In_2Se_3$ has been investigated using micromagnetic simulation. Here, the ferroelectric polarization of In_2Se_3 destroyes the center inversion symmetry of LaCl, while the DMI comes from the strong SOC of the 5d orbit of the rare metal La, which promotes the generation of bimerons [32].

Ferroelectric materials are another branch of materials that can host skyrmions and related spin structures, including so-called 3D skyrmions in the $PbTiO_3$ layer [25], skyrmion-like states in $PbTiO_3$ nanodisks [125] and skyrmionic states in nanocomposites $Ba_{0.15}Sr_{0.85}TiO_3$ [26].

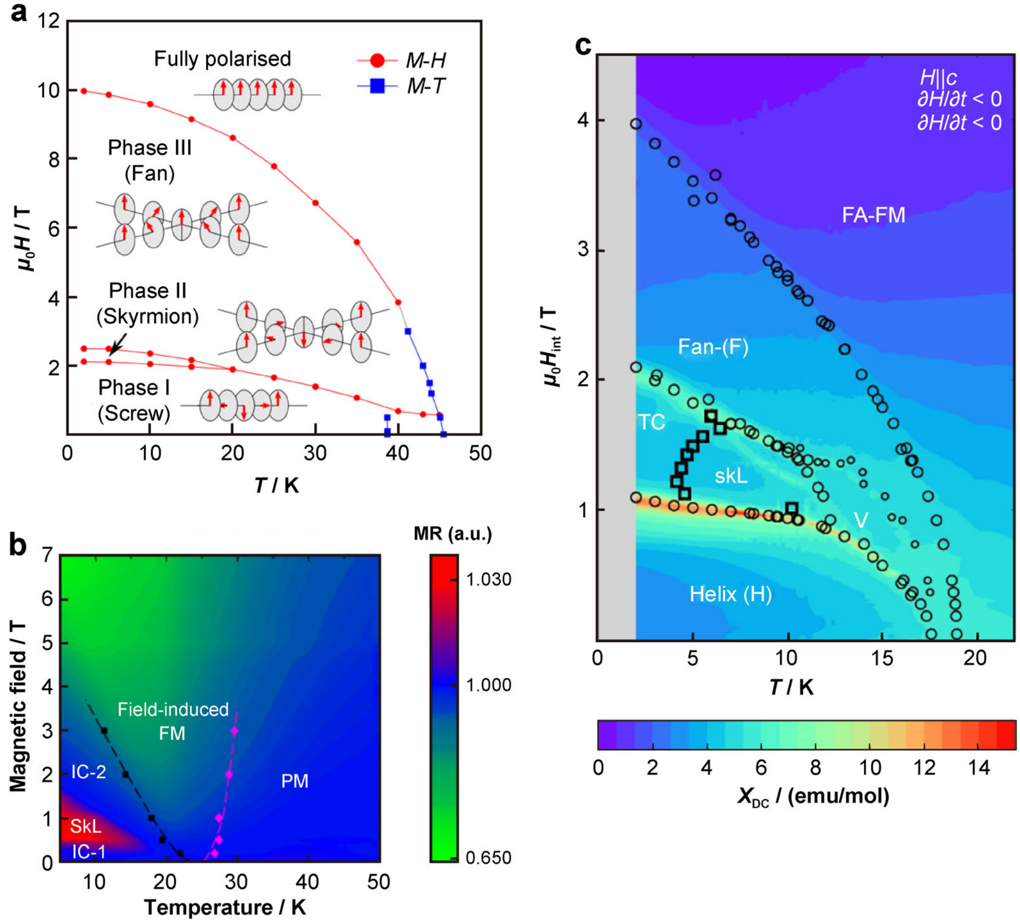

Fig. 6 Phase diagrams of $GdRu_2Si_2$, Gd_2PdSi_3 and $Gd_3Ru_4Al_{12}$ in sequence. **a** Magnetic phase diagram of $GdRu_2Si_2$, where skyrmions can appear below 20 K with a large applied field (> 2 T). Reproduced with permission from Ref. [110]. Copyright 2020, Springer Nature. **b** Contour plot of measured magnetoresistance (MR) of Gd_2PdSi_3, indicating that skL can exist only below 20 K in addition to a magnetic field (0–1.5 T). Reproduced with permission from Ref. [111]. Copyright 2020, IOP Publishing. **c** Contour plot of magnetic susceptibility $\chi_{DC} = \partial M/\partial H$ (where M is bulk magnetization, and H is externally applied magnetic field) of $Gd_3Ru_4Al_{12}$, demonstrating that skyrmions can only survive at low temperatures (below 15 K) and a strong applied field (1.0–1.7 T). Reproduced with permission from Ref. [112]. Copyright 2019, Springer Nature

5.4 Antiskyrmions in Heusler materials

In addition to the above-mentioned topological spin structures, antiskyrmions have also been found recently, which are identified in tetragonal Heusler materials $Mn_{1.4}Pt_{0.9}Pd_{0.1}Sn$ [33], low magnetization ferrimagnet $Mn_2Rh_{0.95}Ir_{0.05}Sn$ [34], Fe/Gd-based multilayers [35] and Co/Pt multilayers [36]. The specific structure of the antiskyrmion generated in $Mn_2Rh_{0.95}Ir_{0.05}Sn$ material is shown in Fig. 7a [34], where the transmitted electron beam converges vertically toward the center of the antiskyrmion and then diverges horizontally. Therefore, in the LTEM image of antiskyrmion, two bright and two dark lobes will form, as shown in Fig. 7a, b. Magnetic phase diagram of $Mn_2Rh_{0.95}Ir_{0.05}Sn$ is shown in Fig. 7c. The rare metal Rh in $Mn_2Rh_{0.95}Ir_{0.05}Sn$ material plays important roles in providing a small DMI, which can stabilize the antiskyrmion at nearly room temperature. Similar LTEM image of antiskyrmions has been observed in the $Mn_{1.4}Pt_{0.9}Pd_{0.1}Sn$ material [33].

6 Generating and manipulating topological spin structures using RE permanent magnets

6.1 Spin-reorientation-related skyrmions in RE permanent magnets

The RE metals can offer strong SOC due to their 4f orbits with underfilling electrons and hence the huge crystalline anisotropy field. This giant crystalline anisotropy in turn provides the large coercivity and thus the great energy

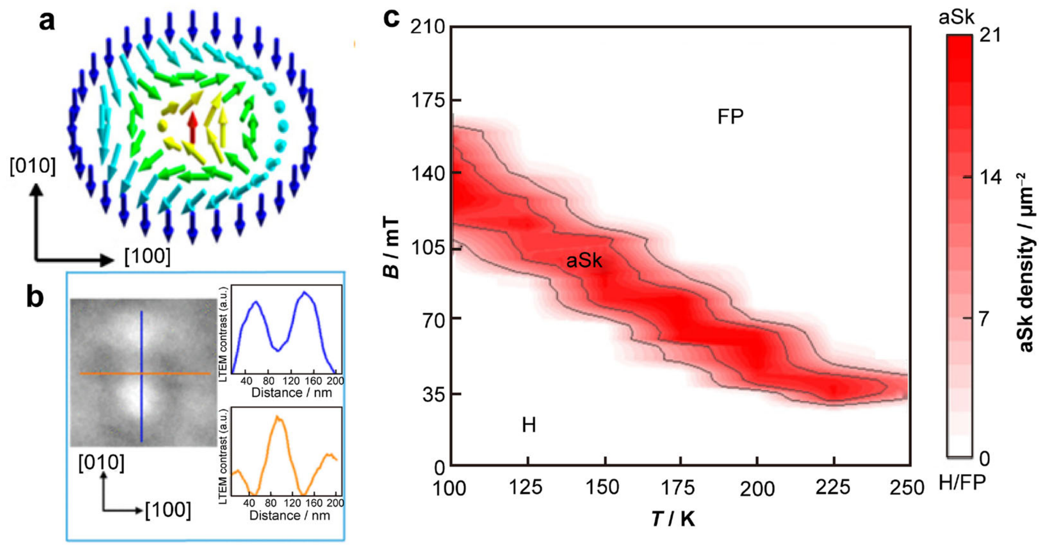

Fig. 7 Schematic diagram of antiskyrmion in $Mn_2Rh_{0.95}Ir_{0.05}Sn$. **a** Distribution of magnetic moment of an antiskyrmion; **b** LTEM image of a single antiskyrmion at 150 K in presence of a magnetic field of 83 mT, where insets being intensity profiles of contrast along [010] (blue color) and [100] (orange color) directions; **c** magnetic phase diagram of $Mn_2Rh_{0.95}Ir_{0.05}Sn$, which shows that antiskyrmions are stable over a wide temperature range of 100–250 K at a suitable magnetic field, where *H,* aSk and FP stand for helical, antiskyrmion and field-polarized states, respectively. Reproduced with permission from Ref. [34]. Copyright 2020, American Chemical Society

products necessary for the permanent magnets [126, 127, 128]. RE permanent magnets normally do not display topological spin structures because of the lack of the DMI. However, on certain special occasions, RE permanent magnets can display skyrmions or vortices states. The first case is associated with the spin reorientation, typically occurring at low temperatures for NdFeB. Xiao et al. [129] observed topologically stable skyrmions in $Nd_2Fe_{14}B$ by LTEM around the spin reorientation temperature (T_{SR}), whereas magnetic bubbles were observed at temperatures higher than T_{SR}. Skyrmions appear because of the tunable anisotropy and saturation magnetization at T_{SR}, which results mainly from the RE metal Nd. The fall in temperature leads to a significant change in the anisotropy constants from positive to negative, which triggers the spin-reorientation, thereby forming the stable skyrmions.

Similar trigger of topological spin structures by spin reorientation in RE-based magnets have been investigated by Hou et al. [130], where $REMn_2Ge_2$ (RE = Ce, Pr, and Nd) can host skyrmionic bubbles in a wide temperature range due to the change of the easy axis. Generally, the topological spin structures are more stable in materials with easy-plane anisotropy than in materials with easy-axis one, leading to the formation of the skyrmions [129] and skyrmionic bubbles [130] near the T_{SR}. Owing to the same reason, skyrmions in GaV_4Se_8 with an easy-plane anisotropy are more stable than those in GaV_4Se_8 with an easy-axis anisotropy [28].

6.2 Generating vortices in hard/soft multilayers

On the other hand, RE permanent magnets can help soft magnetic metals to maintain the vortex state in the demagnetization process, as theoretically demonstrated in NdFeB/FeCo [39], exchange coupled NdFeB/Fe [40] and Sm-Co/Fe multilayers [131] with a perpendicular crystalline anisotropy. However, it should be noted that there is no vortex state reported in the hard/soft multilayers with an in-plane crystalline anisotropy [132–134].

Vortices states can normally occur in the thin films of very soft magnetic materials like permalloy to reduce the demagnetization energy. However, these vortices ultimately disappear, resulting in a full magnetic reversal under a small applied magnetic field due to the limited coercivity originating from very weak crystalline anisotropy. In exchange coupled multilayers, the large perpendicular crystalline anisotropies provided by the RE permanent magnets will pin the vortex in the soft phase so that it will survive in a larger applied field range, as shown in Fig. 8. Similar vortex states have been found in Ref. [40]. These vortices states produced in the soft phase within hard/soft multilayers have not been observed in experiments yet due to the experimental difficulty in separating the signals in hard and soft layers, which becomes more difficult because the soft phase is normally sandwiched between two hard phases. Technically, a hard/soft bilayer can produce the vortex state similar to a multilayer, where the vortex state in the soft phase can be detected relatively easier.

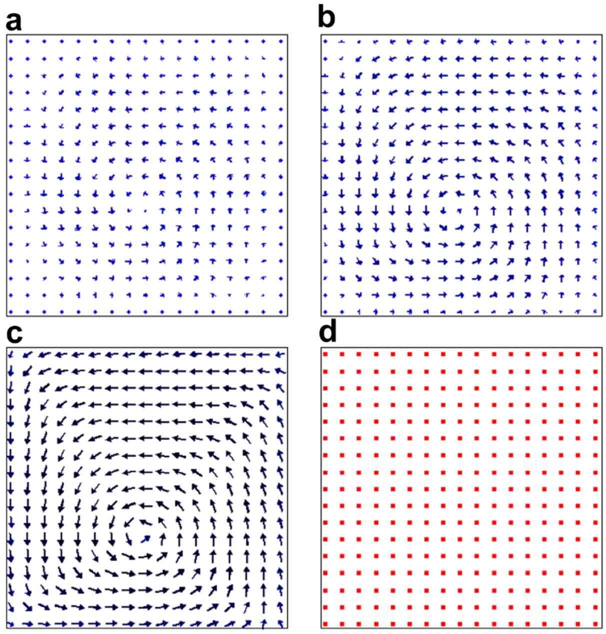

Fig. 8 2D evolution of magnetic moments at hard-soft interface calculated by Mumax3 for a $Nd_2Fe_{14}B$(15 nm)/α-Fe(5 nm) bilayer with a perpendicular anisotropy, which demonstrates nucleation, evolution and annihilation of vortices state. **a** $H = -0.35$ T, formation of vortex magnetic state after nucleation; **b** $H = -0.65$ T, where vortex core begins to rotate away; **c** $H = -1.53$ T, right at coercive point where component of magnetic moment in film plane is the largest; and **d** $H = -1.54$ T, annihilation of vortex state after magnetic reversal

6.3 Setting RE permanent magnets to prevent annihilation of skyrmions in racetracks and nano-oscillators

Another important role played by the RE permanent magnets is to pin the skyrmions in the racetrack center and hence to avoid the annihilation of the skyrmion signal [135]. Driven by the applied current, the skyrmions will be drifted to the CoPt racetrack edge due to the Magnus force. Setting the NdFeB and other RE permanent magnets with huge crystalline anisotropy at the edge provides an additional energy barrier that pushes the skyrmion back to the center of the racetrack. As a result, skyrmions will move along the racetrack stably and avoid the skyrmion signals loss. Interestingly, the skyrmion speed along the racetrack will be increased by 30% in comparison with the case of a normal CoPt racetrack without a setting. An in-depth analysis shows that the settings of the high crystalline anisotropy material at the edge push the transverse speed back to the longitudinal direction, thereby increasing the speed of the skyrmions along the racetrack. Similar idea has been used by Juge et al. [136] and Ohara et al. [137] in experiments to hold skyrmions in Pt/Co/MgO racetracks and $[Pt/CoNi/FeCo]_N$ multilayers, respectively, where the PMA and DMI have been modified by He^+ irradiation [136] or fabricating square and stripe patterns [137]. The PMA and DMI at the edges are enhanced or reduced, hence forming an energy barrier (or trap) to prevent the annihilation of skyrmions at the edges.

Similar enhancement can be applied to a spin-torque nano-oscillator, where RE permanent magnets can be set at the edge of a CoPt disk to avoid the annihilation of the skyrmion signals at the edge. The inlay of the NdFeB at the edge provides an additional energy barrier, pushes back the skyrmion toward the disk center [138], avoids the annihilation of the skyrmion signals and increases the skyrmion frequency by 75%. The noble metal Pt provides the huge SOC and hence the large DMI values necessary for generating skyrmions. On the other hand, the RE metals Nd and Sm provide strong crystalline fields and hence the large PMA, which offer a necessary energy barrier to support skyrmion stability in the CoPt racetrack or the oscillator.

7 Manipulating and generating topological states in antiferromagnets and ferrimagnets

Using the AFM disk, the skyrmion frequency and the related speed in a spin-torque nano-oscillator can be raised by an order. As shown in Fig. 9 [139], the SkHE in an AFM disk disappears naturally so that the skyrmion can rotate steadily around the disk at an ultra-fast speed. Interestingly, the direction of the skyrmion motion is reversed when the current direction switches. In contrast, the skyrmion drifts toward the edge with a negative current while it drifts toward the center with a positive one. For spin-torque nano-oscillators based on ferrimagnetic and AFM skyrmions, the physical mechanisms of their steady motion are different.

AFM materials can also be used in a rectangular racetrack [140], where the AFM skyrmions can be driven efficiently by an anisotropy gradient. Similar to the spin-torque nano-oscillator, the AFM skyrmion speed can be enhanced by one order in comparison with a ferromagnetic skyrmion with the same anisotropy gradient.

AFM skyrmions combine the topology aspect of skyrmions with the fascinating AFM spintronics [141]. The latter has a lot of advantages over the fast-developed ferromagnetic spintronics, namely, much faster dynamics, eliminating the crosstalk between neighboring memory cells due to the disappearance of the net magnetization and multiple stable values via two sets of exchange coupled sublattices [141]. It is also noted that the defects [142] in AFM materials play a more important role in pinning the skyrmions than in ferromagnetic materials. In the latter case, skyrmions can circle around the defects so that the pinning effect around the defects is alleviated. AFM

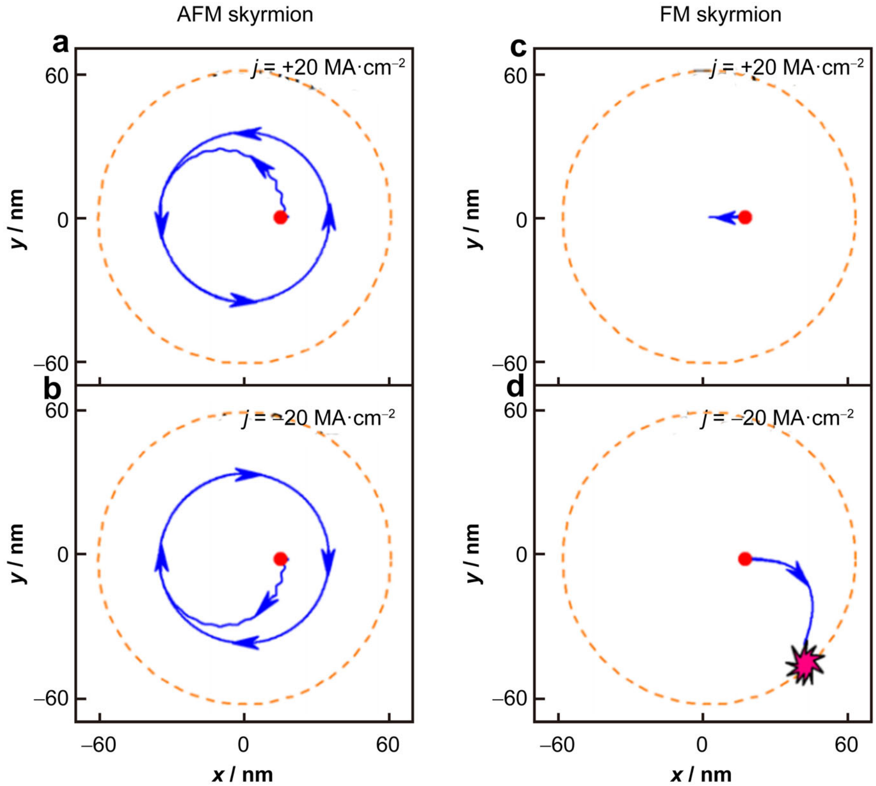

Fig. 9 Motion of AFM and ferrimagnetic skyrmions driven by different currents in nanodisk, where solid lines and dash lines stand for trajectory of skyrmions and nanodisk edges, respectively. An AFM skyrmion driven by a current of **a** j = 20 MA·cm^{-2} and **b** j = –20 MA·cm^{-2}; a ferrimagnetic skyrmion driven by a current of **c** j = 20 MA·cm^{-2} and **d** j = –20 MA·cm^{-2}. Reproduced with permission from Ref. [139]. Copyright 2019, AIP Publishing

skyrmion-based logic gates have been designed, inspired by the pinning of defects in AFM materials [142].

Most works on AFM skyrmions are theoretical, which do not specify the material. In any case, the nontrivial DMI is necessary for the generation of skyrmions, which is usually related to rare metals. Morvan et al. [143] found that skyrmions can form in the ferromagnetic-AFM bilayer based on the micromagnetic calculation. The AFM material adopted is $BiFeO_3$, which is also a multiferroic material. The rare metal Bi here is responsible for regulating both DMI and ferroelectronic behavior of the system.

Besides skyrmions, other topological spin structures can exist stably in AFM materials, including bimerons and half skyrmions [41]. Shen et al. [27] theoretically investigated the dynamics and chaos of AFM bimerons and found that the bimerons can be stable in AFM materials, which is confirmed by the experiment. Based on α-Fe_2O_3 capped with a Pt layer, AFM merons, antimerons and bimerons can emerge from the interface between α-Fe_2O_3 and Pt at room temperature [41], where these spin textures can be tuned by the anisotropy contributed by the rare noble metal Pt. Moreover, the doping of rare metal Rh in a basal α-Fe_2O_3 composite raises the temperature of the Morin transition, above which the complex spin textures are observed. By tuning the additional anisotropy induced by the rare metal overlayer Pt, which changes with the temperature, the authors show that they can control the (anti)meron core size.

Although antiferromagnets demonstrate ultrafast magnetization dynamics, their spin textures are difficult to be detected by electronic methods due to the zero net magnetization. On the other hand, ferrimagnets combine the advantages of both antiferromagnets and ferromagnets, namely, the high mobility and easy detection of skyrmions respectively. Caretta et al. [144] observed 10 nm skyrmions and fast-moving (1.3 km·s^{-1}) domain walls in the ferrimagnetic Pt/$Gd_{44}Co_{56}$/TaO_x, where the rare metals Pt and Gd can help to offer SOT and PMA, separately. Woo et al. [145] found the ferrimagnetic skyrmion with the reduced skyrmion Hall angle and provided a way of the writing and deleting of a single skyrmion in ferrimagnetic GdFeCo films [23]. Particularly, such ferrimagnetic films of amorphous alloys, consisting of 4f RE and 3d transition-metal elements (RE-TM alloys), can exhibit large PMA and host skyrmion states. Besides the single skyrmion mentioned above, the compact ferrimagnetic skyrmions, with a characteristic core radius about 40 nm, have been observed in the other RE-TM alloy, $DyCo_3$ film [146]. In addition, two distinct skyrmion phases are realized in the hybrid ferro/ferri/ferromagnetic multilayer system at room temperature, containing two $[Ir/Fe/Co/Pt]_5$ multilayers separated by the ferrimagnetic $[TbGd/Co]_6$ layer [147]. The ferrimagnetic layer permits an independent adjustment of anisotropy and magnetization by the RE element ratio (Tb:Gd) and RE:TM thickness ratio (TbGd to Co), respectively.

8 Summary and outlook

The important roles of rare metals in generating and manipulating skyrmions and other topological spin structures are reviewed. In general, rare metals can raise the SOC and hence DMI and other related interactions, thereby enhancing the stability of the skyrmions and other topological spin structures. In B20 crystals, rare metal Ge is responsible for the increase of the T_C and expansion of the temperature range in which Bloch-type skyrmions can occur. In thin films and multilayers composed of magnetic and heavy metals, rare metals help to provide considerable PMA or four spin interactions, in addition to strong DMI necessary for the emergence of Néel-type skyrmions. In frustrated materials, rare metals can offer the RKKY interaction or the competing ferrimagnetic and AFM exchange interactions to stabilize skyrmions. Moreover, rare metals can provide additional magnetocrystalline anisotropy and magnetic moments in various materials and trigger the formation of skyrmions and other topological spin structures. In particular, the appearance of skyrmions in $Nd_2Fe_{14}B$ and GaV_4Se near T_{SR} is due to the abrupt change in the magnetocrystalline anisotropy and magnetic moments. This offers a new approach to search for novel materials generating skyrmions, i.e., the materials with spin reorientation where the crystalline anisotropy changes from the uniaxial to an easy plane.

Rare metals can also help to provide additional energy barrier or RKKY interaction to curb or cancel the SkHE and avoid the annihilation of signals in a skyrmion-based racetrack [20–22, 134]. Similar designs can be extended to skyrmion-based logic gates [148], nano-oscillators [149], diodes [150], transistors [151] and neuromorphic computing [152]. In addition, compared with the method driven by the current, the manipulation of exotic topological spin structures by the electric field is getting more and more attention and possess a strong potential to realize next-generation low-consumption spintronics [153, 154]. Therefore, rare metals can play more important roles in manipulating the dynamics of skyrmions in the future.

Acknowledgements This work was financially supported by the National Natural Science Foundation of China (Nos. 51771127, 52171188 52111530143, 12104327, 51901081, 11974298 and 61961136006), the National Key Research and Development Program of China (No. 2020YFA0309300), Sichuan Science and Technology Program (Application No. 21ZYZYTS0077), the Science and Technology Program of Guangzhou (No. 202002030052), Guangdong Special Support Project (No. 2019BT02X030), Shenzhen Fundamental Research Fund (No. JCYJ20210324120213037), Shenzhen Peacock Group Plan (No. KQTD20180413181702403), Pearl River Recruitment Program of Talents (No. 2017GC010293) and the Grants-in-Aid for Scientific Research from JSPS KAKENHI (Nos. JP20F20363, JP21H01364 and JP21K18872).

Declarations

Conflict of interests The authors declare that they have no conflict of interest.

References

[1] Skyrme THR. A unified field theory of mesons and baryons. Nucl Phys. 1962;31:556.
[2] Bongdnov N, Yablonskii DA. Thermodynamically stable "vortices" in magnetically ordered crystals. The mixed state of magnets. Sov Phys JETP. 1989;68:101.
[3] Mühlbauer S, Binz B, Jonietz F, Pfleiderer C, Rosch A, Neubauer A, Georgii R, Böni P. Skyrmion lattice in a chiral magnet. Science. 2009;323(5916):915.
[4] Yu XZ, Onose Y, Kanazawa N, Park JH, Han JH, Matsui Y, Nagaosa N, Tokura Y. Real-space observation of a two-dimensional skyrmion crystal. Nature. 2010;465(7300):901.
[5] Peng LC, Zhang Y, Zuo SL, He M, Cai JW, Wang SG, Wei HX, Li JQ, Zhao TY, Shen BG. Lorentz transmission electron microscopy studies on topological magnetic domains. Chin Phys B. 2018;27(6):066802.
[6] Tanigaki T, Shibata K, Kanazawa N, Yu XZ, Onose Y, Park HS, Shindo D, Tokura Y. Real-space observation of short-period cubid lattice of skyrmions in MnGe. Nano Lett. 2015;15(8):5438.
[7] Yu XZ, Kanazawa N, Onose Y, Kimoto K, Zhang WZ, Ishiwata S, Matsui Y, Tokura Y. Near room-temperature formation of a skyrmion crystal in thin-films of the helimagnet FeGe. Nat Mater. 2011;10(2):106.
[8] Fert A, Cros V, Sampaio J. Skyrmions on the track. Nat Nanotech. 2013;8(3):152.
[9] Jl G, Rugar AE, Ralph DC. Creation of localized skyrmion bubbles in Co/Pt bilayers using a spin-valve nanopillar. Phys Rev B. 2018;97(18):184424.
[10] Jiang WJ, Upadhyaya P, Zhang W, Yu GQ, Jungfleisch MB, Fradin FY, Pearson JE, Tserkovnyak Y, Wang KL, Heinonen O, Velthuis SGE, Hoffmann A. Blowing magnetic skyrmion bubbles. Science. 2015;349(6245):283.
[11] Yu GQ, Upadhyaya P, Li X, Li WY, Kim SK, Fan YB, Wong KL, Tserkovnyak Y, Amiri PK, Wang KL. Room-temperature creation and spin-orbit torque manipulation of skyrmions in thin films with engineered asymmetry. Nano Lett. 2016;16(3):1981.
[12] Yan ZR, Liu YZ, Guang Y, Feng JF, Lake RK, Yu GQ, Han XF. Robust skyrmion shift device through engineering the local exchange-bias field. Phys Rev Appl. 2020;14(4):044008.
[13] Yu GQ, Jenkins A, Ma X, Razavi SA, He CL, Yin G, Shao QM, He QL, Wu H, Li WJ, Jiang WJ, Han XF, Li XQ, Jayich ACB, Amiri PK, Wang KL. Room-temperature skyrmions in an antiferromagnet-based heterostructure. Nano Lett. 2018;18(2):980.

[14] Zeissler K, Mruczkiewicz M, Finizio S, Raabe J, Shepley PM, Sadovnikov AV, Nikitov SA, Fallon K, McFadzean S, McVitie S, Moore TA, Burnell G, Marrows CH. Pinning and hysteresis in the field dependent diameter evolution of skyrmions in Pt/Co/Ir superlattice stacks. Sci Rep. 2017;7:15125.
[15] Wang L, Liu C, Mehmood N, Han G, Wang YD, Xu XL, Feng C, Hou ZP, Peng Y, Gao XS, Yu GH. Construction of a room-temperature Pt/Co/Ta multilayer film with ultrahigh-density skyrmions for memory application. ACS Appl Mater Interf. 2019;11(12):12098.
[16] Tejo F, Velozo F, Elias RG, Escrig J. Oscillations of skyrmion clusters in Co/Pt multilayer nanodots. Sci Rep. 2020;10(1):16517.
[17] Moreau-Luchaire C, Moutafis C, Reyren N, Sampaio J, Vaz CAF, Van Horne N, Bouzehouane K, Garcia K, Deranlot C, Wohlhuter P, George JM, Weigand M, Raabe J, Cros V, Fert A. Additive interfacial chiral interaction in multilayers for stabilization of small individual skyrmions at room temperature. Nat Nanotech. 2016;11(5):444.
[18] Yang HX, Thiaville A, Rohart S, Fert A, Chshiev M. Anatomy of Dzyaloshinskii-Moriya interaction at Co/Pt interfaces. Phys Rev Lett. 2015;115(26):267210.
[19] Boulle O, Vogel J, Yang HX, Pizzini S, Chaves DD, Locatelli A, Mentes TO, Sala A, Buda-Prejbeanu LD, Klein O, Belmeguenai M, Roussigne Y, Stashkevich A, Cherif SM, Aballe L, Foerster M, Chshiev M, Auffret S, Miron IM, Gaudin G. Room-temperature chiral magnetic skyrmions in ultrathin magnetic nanostructures. Nat Nanotech. 2016;11(5):449.
[20] Zhang XC, Zhou Y, Ezawa M. Magnetic bilayer-skyrmions without skyrmion Hall effect. Nat Commun. 2016;7:10293.
[21] Chen RY, Gao Y, Zhang XC, Zhang RQ, Yin SQ, Chen XZ, Zhou XF, Zhou YJ, Xia J, Zhou Y, Wang SG, Pan F, Zhang Y, Song C. Realization of isolated and high-density skyrmions at room temperature in uncompensated synthetic antiferromagnets. Nano Lett. 2020;20(5):3299.
[22] Zhang JY, Zhang Y, Gao Y, Zhao GP, Qiu L, Wang KY, Dou PW, Peng WL, Zhuang Y, Wu YF, Yu GQ, Zhu ZZ, Zhao YC, Guo YQ, Zhu T, Cai JW, Shen BG, Wang SG. Magnetic skyrmions in a hall balance with interfacial canted magnetizations. Adv Mater. 2020;32(28):1907452.
[23] Woo S, Song KM, Zhang XC, Zhou Y, Ezawa M, Liu XX, Finzio S, Raabe J, Lee NJ, Kim SI, Park SY, Kim Y, Kim JY, Lee D, Lee O, Choi JW, Min BC, Koo HC, Chang J. Current-driven dynamics and inhibition of the skyrmion Hall effect of ferrimagnetic skyrmions in GdFeCo films. Nat Commun. 2018;9:959.
[24] Zhang HM, Chen J, Barone P, Yamauchi K, Dong S, Picozzi S. Possible emergence of a skyrmion phase in ferroelectric $GaMo_4S_8$. Phys Rev B. 2019;99(21):214427.
[25] Das S, Tang YL, Hong Z, Gonçalves MAP, McCarter MR, Klewe C, Nguyen KX, Gómez-Ortiz F, Shafer P, Arenholz E, Stoica VA, Hsu SL, Wang B, Ophus C, Liu JF, Nelson CT, Saremi S, Prasad B, Mei AB, Schlom DG, Íñiguez J, García-Fernández P, Muller DA, Chen LQ, Junquera J, Martin LW, Ramesh R. Observation of room-temperature polar skyrmions. Nature. 2019;568(7752):368.
[26] Nahas Y, Prokhorenko S, Louis L, Gui Z, Kornev I, Bellaiche L. Discovery of stable skyrmionic state in ferroelectric nanocomposites. Nat Commun. 2015;6:8542.
[27] Shen LC, Xia J, Zhang XC, Ezawa M, Tretiakov OA, Liu XX, Zhao GP, Zhou Y. Current-induced dynamics and chaos of antiferromagnetic bimerons. Phys Rev Lett. 2020;124:037202.
[28] Kezsmarki I, Bordacs S, Milde P, Neuber E, Eng LM, White JS, Rønnow HM, Dewhurst CD, Mochizuki M, Yanai K, Nakamura H, Ehlers D, Tsurkan V, Loidl A. Néel-type skyrmion lattice with confined orientation in the polar magnetic semiconductor GaV_4S_8. Nat Mater. 2015;14(11):1116.
[29] Zhou Y, Wei W, Zhang B, Yuan Y, Chen C, Chen X, An C, Zhou Y, Wu H, Wang S, Qi M, Zhang R, Park C, Tian M, Yang Z. Effect of pressure on structural and electronic properties of the noncentrosymmetric superconductor Rh_2Mo_3N. Phys Rev B. 2019;100(17):174516.
[30] Ding B, Li ZF, Xu GZ, Li H, Hou ZP, Liu E, Xi XK, Xu F, Yao Y. Observation of magnetic skyrmion bubbles in a Van Der Waals ferromagnet Fe_3GeTe_2. Nano Lett. 2020;20(2):868.
[31] Wu YY, Zhang SF, Zhang JW, Wang W, Zhu YL, Hu J, Yin G, Wong K, Fang C, Wan CH, Han XF, Shao QM, Taniguchi TK, Watanabe KJ, Zang JD, Mao ZQ, Zhang XX, Wang KL. Néel-type skyrmion in WTe_2/Fe_3GeTe_2 Van Der Waals heterostructure. Nat Commun. 2020;11:3860.
[32] Sun W, Wang WX, Li H, Zhang GB, Chen D, Wang JL, Cheng ZX. Controlling bimerons as skyrmion analogues by ferroelectric polarization in 2D Van Der Waals multiferroic heterostructures. Nat Commun. 2020;11(1):5930.
[33] Nayak AK, Kumar V, Ma TP, Werner P, Pippel E, Sahoo R, Damay F, Rößler UK, Felser C, Parkin SSP. Magnetic antiskyrmions above room temperature in tetragonal Heusler materials. Nature. 2017;548(7669):561.
[34] Jena J, Stinshoffff R, Saha R, Srivastava AK, Ma T, Deniz H, Werner P, Felser C, Parkin SSP. Observation of magnetic antiskyrmions in the low magnetization ferrimagnet $Mn_2Rh_{0.95}Ir_{0.05}Sn$. Nano Lett. 2020;20(1):59.
[35] Heigl M, Koraltan S, Vaňatka M, Kraft R, Abert C, Vogler C, Semisalova A, Che P, Ullrich A, Schmidt T, Hintermayr J, Grundler D, Farle M, Urbánek M, Suess D, Albrecht M. Dipolar-stabilized first and second-order antiskyrmions in ferrimagnetic multilayers. Nat Commun. 2021;12:2611.
[36] Zhang S, Petford-Long AK, Phatak C. Creation of artificial skyrmions and antiskyrmions by anisotropy engineering. Sci Rep. 2016;6:31248.
[37] Zhang XC, Xia J, Shen LC, Ezawa M, Tretiakov OA, Zhao GP, Liu XX, Zhou Y. Static and dynamic properties of bimerons in a frustrated ferromagnetic monolayer. Phys Rev B. 2020;101(14):144435.
[38] Xia J, Zhang XC, Ezawa M, Tretiakov OA, Hou ZP, Wang WH, Zhao GP, Liu XX, Diep HT, Zhou Y. Current-driven skyrmionium in a frustrated magnetic system. Appl Phys Lett. 2020;117(1):012403.
[39] Peng Y, Zhao GP, Wu SQ, Si WJ, Wan XL. Micromagnetic simulation and analysis of $Nd_2Fe_{14}B/Fe_{65}Co_{65}$ magnetic bilayered thin films with different orientations of the easy axis. Acta Phys Sin-Ched. 2014;63(16):167505.
[40] Yuan XH, Zhao GP, Yue M, Ye LN, Xia J, Zhang XC, Chang J. 3D and 1D calculation of hysteresis loops and energy products for anisotropic nanocomposite films with perpendicular anisotropy. J Magn Magn Mater. 2013;343:245.
[41] Jani H, Lin JC, Chen JH, Harrison J, Maccherozzi F, Schad J, Prakash S, Eom CB, Ariando A, Venkatesan T, Radaelli PG. Antiferromagnetic half-skyrmions and bimerons at room temperature. Nature. 2021;590(7844):74.
[42] Kent N, Reynolds N, Raftrey D, Campbell LTG, Virasawmy S, Dhuey S, Chopdekar RV, Hierro-Rodriguez A, Sorrentino A, Pareiro E, Ferrer S, Hellman F, Sutcliffe P, Fischer P. Creation and observation of Hopfions in magnetic multilayer systems. Nat Commun. 2021;12:1562.
[43] Tang J, Wu YD, Wang WW, Kong LY, Lv B, Wei WS, Zang JD, Tian ML, Du HF. Magnetic skyrmion bundles and their current-driven dynamics. Nat Nanotech. 2021. https://doi.org/10.1038/s41565-021-00954-9.
[44] Nagaosa N, Tokura Y. Topological properties and dynamics of magnetic skyrmions. Nat Nanotechnol. 2013;8(12):899.

[45] von Bergmann K, Kubetzka A, Pietzsch O, Woesendanger R. Interface-induced chiral domain walls, spin spirals and skyrmions revealed by spin-polarized scanning tunneling microscopy. J Phys Condens Matter. 2014;26(39):394002.
[46] Zhang ZD. Magnetic structures, magnetic domains and topological magnetic textures of magnetic materials. Acta Physica Sinica. 2015;64(6):067503.
[47] Wiesendanger R. Nanoscale magnetic skyrmions in metallic films and multilayers: a new twist for spintronic. Nat Rev Mater. 2016;1(7):16044.
[48] Finocchio G, Buttner F, Tomasello R, Carpentieri M, Klaui M. Magnetic skyrmions: from fundamental to applications. J Phys D. 2016;49(42):423001.
[49] Fert A, Reyren N, Cros V. Magnetic skyrmions: advances in physics and potential applications. Nat Rev Mater. 2017;2(7): 17031.
[50] Hellman F, Hoffmann A, Tserkovnyak Y, Beach GSD, Fullerton EE, Leighton C, MacDonald AH, Ralph DC, Arena DA, Durr HA, Fischer P, Grollier J, Heremans JP, Jungwirth T, Kimel AV, Koopmans B, Krivorotov IN, May SJ, Petford-Long AK, Rondinelli JM, Samarth N, Schuller IK, Slavin AN, Stiles MD, Tchernyshyov O, Thiaville A, Zink BL. Interface-induced phenomena in magnetism. Rev Mod Phys. 2017;89(2):25006.
[51] Jiang WJ, Chen G, Liu K, Zang JD, te Velthuis SGE, Hoffmann A. Skyrmion in magnetic multilayers. Phys Rep. 2017; 704:1.
[52] Liang X, Zhao L, Qiu L, Li S, Ding LH, Feng YH, Zhang XC, Zhou Y, Zhao GP. Skyrmions-based magnetic racetrack memory. Acta Physica Sinica. 2018;67(13):137510.
[53] Zhou Y. Mangetic skyrmions: intriguing physics and new spintronic device concepts. Natl Sci Rev. 2019;6(2):210.
[54] Zhang XC, Zhou Y, Song KM, Park TE, Xia J, Ezawa M, Liu XX, Zhao WS, Zhao GP, Woo S. Skyrmion-electronics: writing, deleting, reading and processing magnetic skyrmions toward spintronic applications. J Phys Condens Matter. 2020; 32(14):143001.
[55] Gobel B, Merting I, Tretiakov OA. Beyond skyrmions: review and perspectives of alternative magnetic quasiparticles. Phys Rep. 2021;895:1.
[56] Grigoriev SV, Dyadkin VA, Moskvin EV, Lamago D, Wolf T, Eckerlebe H, Maleyev H. Helical spin structure of $Mn_{1-y}Fe_ySi$ under a magnetic field: small angle neutron diffraction study. Phys Rev B. 2009;79(14):144417.
[57] Shibata K, Yu XZ, Hara T, Morikawa D, Kanazawa N, Kimoto K, Ishiwata S, Matsui Y, Tokura Y. Towards control of the size and helicity of skyrmions in helimagnetic alloys by spin-orbit coupling. Nat Nanotech. 2013;8(10):723.
[58] Fujima Y, Abe N, Tokunaga Y, Arima T. Thermodynamically stable skyrmion lattice at low temperatures in a bulk crystal of lacunar spinel GaV_4Se_8. Phys Rev B. 2017;95(18):180410.
[59] Schueller EC, Kitchaev DA, Zuo JL, Bocarsly JD, Cooley JA, Van der Ven A, Wilson SD, Seshadri R. Structural evolution and skyrmionic phase diagram of the lacunar spinel $GaMo_4Se_8$. Phys Rev Mater. 2020;4(6):064402.
[60] Li W, Jin C, Che R, Wei W, Lin L, Zhang L, Du H, Tian M, Zang J. Emergence of skyrmions from rich parent phases in the molybdenum nitrides. Phys Rev B. 2016; 93(6):060409(R).
[61] Bordacs S, Butykai A, Szigeti BG, White JS, Cubitt R, Leonov AO, Widmann S, Ehlers D, von Nidda HAK, Tsuikan V, Loidl A, Kezsmarki I. Equilibrium skyrmion lattice ground state in a polar easy-plane magnet. Sci Rep. 2017;7:7584.
[62] Kanazawa N, Seki S, Tokura Y. Noncentrosymmetric magnets hosting magnetic skyrmions. Adv Mater. 2017;29(25): 1603227.
[63] Wei WS, He ZD, Qu Z, Du HF. Dzyaloshinsky-Moriya interaction (DMI)-induced magnetic skyrmion materials. Rare Met. 2021;40(11):3076.
[64] Fert AR. Magnetic and transport properties of metallic multilayers. Mater Sci Forum. 1990;59–60:439.
[65] Bogdanov A, Hubert A. Thermodynamically stable magnetic vortex states in magnetic crystals. J Magn Magn Mater. 1994; 138(3):255.
[66] Roessler UK, Bogdanov AN, Pfleiderer C. Spontaneous skyrmion ground states in magnetic metals. Nature. 2006; 442(7104):797.
[67] Kim S, Ueda K, Go G, Jang PH, Lee KJ, Belabbes A, Manchon A, Suzuki M, Kotani Y, Nakamura T, Nakamura K, Koyama T, Chiba D, Yamada KT, Kim DH, Moriyama T, Kim KJ, Ono T. Correlation of the Dzyaloshinskii-Moriya interaction with Heisenberg exchange and orbital asphericity. Nat Commun. 2018;9:1648.
[68] Heinze S, von Bergmann K, Menzel M, Brede J, Kubetzka A, Wiesendanger R, Bihlmayer G, Blügel S. Spontaneous atomic-scale magnetic skyrmion lattice in two dimensions. Nat Phys. 2011;7(9):713.
[69] Paul S, Haldar S, von Malottki S, Heinze S. Role of higher-order exchange interactions for skyrmion stability. Nat Commun. 2020;11(1):4756.
[70] Grenz J, Köhler A, Schwarz A, Wiesendanger R. Probing the nano-skyrmion lattice on Fe/Ir(111) with magnetic exchange force microscopy. Phys Rev Lett. 2017;119(4):047205.
[71] Hagemeister J, Iaia D, Vedmedenko EY, von Bergmann K, Kubetzka A, Wiesendanger R. Skyrmions at the edge: confinement effects in Fe/Ir(111). Phys Rev Lett. 2016;117(20): 207202.
[72] Dupé M, Heinze S, Sinova J, Dupé B. Stability and magnetic properties of Fe double layers on Ir (111). Phys Rev B. 2018; 98(22):224415.
[73] Hsu PJ, Kubetzka A, Finco A, Romming N, von Bergmann K, Wiesendanger R. Electric-field-driven switching of individual magnetic skyrmions. Nat Nanotech. 2017;12(2):123.
[74] Romming N, Hanneken C, Menzel M, Bickel JE, Wolter B, von Bergmann K, Kubetzka A, Wiesendanger R. Writing and deleting single magnetic skyrmions. Science. 2013;341(6146): 636.
[75] Zhao L, Wang ZD, Zhang XC, Liang X, Xia J, Wu KY, Zhou HA, Dong YQ, Yu GQ, Wang KL, Liu XX, Zhou Y, Jiang WJ. Topology-dependent Brownian gyromotion of a single skyrmion. Phys Rev Lett. 2020;125(2):027206.
[76] Iskin M. Spin-orbit-coupling-induced Fulde-Ferrell-Larkin-Ovchinnikov-like cooper pairing and skyrmion-like polarization textures in optical lattices. Phys Rev A. 2013; 88(1):013631.
[77] Montoya SA, Couture S, Chess JJ, Lee JCT, Kent N, Henze D, Sinha SK, Im MY, Kevan SD, Fischer P, McMorran BJ, Lomakin V, Roy S, Fullerton EE. Tailoring magnetic energies to form dipole skyrmions and skyrmion lattices. Phys Rev B. 2017;95(2):024415.
[78] Soumyanarayanan A, Raju M, Oyarce ALG, Tan AKC, Im MY, Petrović AP, Ho P, Khoo KH, Tran M, Gan CK, Ernult F, Panagopoulos C. Tunable room-temperature magnetic skyrmions in Ir/Fe/Co/Pt multilayers. Nat Mater. 2017;16(9):898.
[79] Belabbes A, Bihlmayer G, Blügel S, Manchon A. Oxygen-enabled control of Dzyaloshinskii-Moriya interaction in ultra-thin magnetic films. Sci Rep. 2016;6:24634.
[80] Zeissler K, Finizio S, Shahbazi K, Massey J, Al Ma'Mari F, Bracher DM, Kleibert A, Rosamond MC, Linfield EH, Moore TA, Raabe J, Burnell G, Marrows CH. Discrete Hall resistivity contribution from Néel skyrmions in multilayer nanodiscs. Nat Nanotech. 2018;13(12):1161.

[81] Hrabec A, Porter NA, Wells A, Benitez MJ, Burnell G, McVitie S, McGrouther D, Moore TA, Marrows CH. Measuring and tailoring the Dzyaloshinskii-Moriya interaction in perpendicularly magnetized thin films. Phys Rev B. 2014;90(2):020402.

[82] Perini M, Meyer S, Dupé B, Malottki SV, Kubetzka A, Bergmann K, Wiesendanger R, Heinze S. Domain walls and Dzyaloshinskii-Moriya interaction in epitaxial Co/Ir(111) and Pt/Co/Ir(111). Phys Rev B. 2018;97(18):184425.

[83] Belabbes A, Bihlmayer G, Bechstedt F, Blügel S, Manchon A. Hund's rule-driven Dzyaloshinskii-Moriya interaction at 3d–5d interfaces. Phys Rev Lett. 2016;117(24):247202.

[84] Vida GJ, Simon E, Rozsa L, Palotas K, Szunyogh L. Domain-wall profiles in Co/Ir n/Pt(111) ultrathin films: influence of the Dzyaloshinskii-Moriya interaction. Phys Rev B. 2016;94(21):214422.

[85] Ryu KS, Yang SH, Thomas L, Parkin SSP. Chiral spin torque arising from proximity-induced magnetization. Nat Commun. 2014;5:3910.

[86] Shahbazi K, Kim JV, Nembach HT, Shaw JM, Bischof A, Rossell MD, Jeudy V, Moore TA, Marrows CH. Domain-wall motion and interfacial Dzyaloshinskii-Moriya interactions in Pt/Co/Ir(t_{Ir})/Ta multilayers. Phys Rev B. 2019;99(9):094409.

[87] Ishikuro Y, Kawaguchi M, Kato N, Lau YC, Hayashi M. Dzyaloshinskii-Moriya interaction and spin-orbit torque at the Ir/Co interface. Phys Rev B. 2019;99(13):134421.

[88] Woo S, Song KM, Han HS, Jung MS, Im MY, Lee KS, Song KS, Fischer P, Hong JI, Choi JW, Min BC, Koo HC, Chang J. Spin-orbit torque-driven skyrmion dynamics revealed by time-resolved X-ray microscopy. Nat Commun. 2017;8:15573.

[89] Peng LC, Takagi R, Koshibae W, Shibata K, Nakajima K, Arima TH, Naoto N, Shinichiro S, Yu XZ, Tokura Y. Controlled transformation of skyrmions and antiskyrmions in a non-centrosymmetric magnet. Nat Nanotechonol. 2020;15:181.

[90] Albisetti E, Petti D, Pancaldi M, Madami M, Tacchi S, Curtis J, King WP, Papp A, Csaba G, Porod W, Vavassori P, Riedo E, Bertacco R. Nanopatterning reconfigurable magnetic landscapes via thermally assisted scanning probe lithography. Nat Nanotech. 2016;11(6):545.

[91] Albisetti E, Petti D, Madami M, Tacchi S, Vavassori P, Riedo E, Bertacco R. Nanopatterning spin-textures: a route to reconfigurable magnonics. AIP Adv. 2016;7(5):055601.

[92] Guang Y. Creating zero-field skyrmions in exchangebiased multilayers through X-ray illumination. Nat Commun. 2020;11(1):949.

[93] Zhang XC, Zhou Y, Ezawa M. Antiferromagnetic skyrmion: stability, creation and manipulation. Sci Rep. 2016;6:24795.

[94] Barker J, Tretiakov OA. Static and dynamical properties of antiferromagnetic skyrmions in the presence of applied current and temperature. Phys Rev Lett. 2016;116(14):147203.

[95] Purnama I, Gan WL, Wong DW, Lew WS. Guided current-induced skyrmion motion in 1D potential well. Sci Rep. 2015;5:10620.

[96] Fook HT, Gan WL, Purnama I, Lew WS. Mitigation of Magnus force in current-induced skyrmion dynamics. IEEE Trans Magn. 2015;51(11):1500204.

[97] Liu JP, Zhang ZD, Zhao GP. Skyrmions: topological structures, properties, and applications. Boca Raton: CRC Press; 2016. 1.

[98] Zhang Y, Luo SJ, Yan BQ, Ouyang J, Yang XF, Chen S, Zhu BP, You L. Magnetic skyrmions without the skyrmion Hall effect in a magnetic nanotrack with perpendicular anisotropy. Nanoscale. 2017;9:10212.

[99] Shen LC, Li XG, Xia J, Qiu L, Zhang XC, Tretiakov OA, Ezawa M, Zhou Y. Dynamics of ferromagnetic bimerons driven by spin currents and magnetic fields. Phys Rev B. 2020;102:104427.

[100] Casiraghi A, Corte-León H, Vafaee M, Garcia-Sanchez F, Durin G, Pasquale M, Jakob G, Kläui M, Kazakova O. Individual skyrmion manipulation by local magnetic field gradients. Commun Phys. 2018;2:145.

[101] Jiang YY, Yuan HY, Li ZX, Wang ZY, Zhang HW, Cao YS, Yan P. Twisted magnon as a magnetic tweezer. Phys Rev Lett. 2020;124:217204.

[102] Zhang GF, Tian Y, Deng YB, Jiang DC, Deng SG. Spin-wave-driven skyrmion motion in magnetic nanostrip. J Nanotechnol. 2018;2018:2602913.

[103] Li S, Xia J, Zhang XC, Ezawa M, Kang W, Liu XX, Zhou Y, Zhao WS. Dynamics of a magnetic skyrmionium driven by spin waves. Appl Phys Lett. 2018;112:142404.

[104] Wang ZD, Guo MH, Zhou HA, Zhao L, Xu T, Tomasello R, Bai H, Dong YQ, Je SG, Chao WL, Han HD, Lee S, Lee KS, Yao YY, Han W, Song C, Wu HQ, Carpentieri M, Finicchio G, Im MY, Lin SZ, Jiang WJ. Thermal generation, manipulation and thermoelectric detection of skyrmions. Nat Electron. 2020;3:672.

[105] Qin PX, Yan H, Wang XN, Feng ZX, Guo HX, Zhou XR, Wu HJ, Leng ZGG, Chen HY, Liu ZQ. Nincollinear spintronics and electric-field control: a review. Rare Met. 2020;39(2):95.

[106] White JS, Levatić I, Omrani AA, Egetenmeyer N, Prša K, Živković I, Gavilano JL, Kohlbrecher J, Bartkowiak M, Berger H, Rønnow HM. Electric field control of the skyrmion lattice in Cu_2OSeO_3. J Phys-Condens Matter. 2012;24(43):432201.

[107] Kruchkov AJ, White JS, Bartkowiak M, Živković I, Magrez A, Rønnow HM. Direct electric field control of the skyrmion phasein a magnetoelectric insulator. Sci Rep. 2018;8:10466.

[108] Nakatani Y, Hayashi Kanai S, Fukami S, Ohno H. Electric field control of skyrmions in magnetic nanodisks. Appl Phys Lett. 2016;108(15):152403.

[109] Ma C, Zhang XC, Xia J, Ezawa M, Jiang WJ, Ono T, Piramanayagam SN, Morisako A, Zhou Y, Liu XX. Electric field-induced creation and directional motion of domain walls and skyrmion bubbles. Nano Lett. 2019;19(1):353.

[110] Yasui Y, Butler CJ, Khanh ND, Hayami S, Nomoto T, Hanaguri T, Motome Y, Arita R, Arima TH, Tokura Y, Seki S. Imaging the coupling between itinerant electrons and localised moments in the centrosymmetric skyrmion magnet $GdRu_2Si_2$. Nat Commun. 2020;11(1):5925.

[111] Zhang H, Huang Q, Hao L, Yang JY, Noordhoek K, Pandey S, Zhou HD, Liu J. Anomalous magnetoresistance in centrosymmetric skyrmion-lattice magnets Gd_2PdSi_3. New J Phys. 2020;22:083056.

[112] Hirschberger M, Nakajima T, Gao S, Peng LC, Kikkawa A, Kurumaji T, Kriener M, Yamasaki Y, Sagayama H, Nakao H, Ohishi K, Kakurai K, Taguchi Y, Yu XZ, Arima TH, Tokura Y. Skyrmion phase and competing magnetic orders on a breathing kagomé lattice. Nat Commun. 2019;10(1):5831.

[113] Hou ZP, Ren WJ, Ding B, Xu GZ, Wang Y, Yang B, Zhang Q, Zhang Y, Liu E, Xu F, Wang WH, Wu GH, Zhang XX, Shen B, Zhang Z. Observation of various and spontaneous magnetic skyrmionic bubbles at room temperature in a frustrated kagome magnet with uniaxial magnetic anisotropy. Adv Mater. 2017;29(29):1701144.

[114] Hou ZP, Zhang Q, Xu GZ, Gong C, Ding B, Wang Y, Li H, Liu E, Xu F, Zhang HW, Yao Y, Wu GH, Zhang XX, Wang WH. Creation of single chain of nanoscale skyrmion bubbles with record-high temperature stability in a geometrically confined nanostripe. Nano Lett. 2018;18(2):1274.

[115] Hou ZP, Zhang Q, Xu GZ, Zhang SF, Gong C, Ding B, Li H, Xu F, Yao Y, Liu E, Wu GH, Zhang XX, Wang WH. Manipulating the topology of nanoscale skyrmion bubbles by spatially geometric confinement. ACS Nano. 2019;13(1):922.

[116] Hou ZP, Zhang Q, Zhang XC, Xu GZ, Xia J, Ding B, Li H, Zhang SF, Batra NM, Costa PMFJ, Liu E, Wu GH, Ezawa M, Liu XX, Zhou Y, Zhang XX, Wang WH. Current-induced helicity reversal of a single skyrmionic bubble chain in a nanostructured frustrated magnet. Adv Mater. 2020;32(1): 1904815.
[117] Zhang XC, Xia J, Ezawa M, Tretiakov OA, Diep HT, Zhao GP, Liu XX, Zhou Y. A frustrated bimeronium: static structure and dynamics. Appl Phys Lett. 2021;118(5):052411.
[118] Bettler S, Landolt F, Aksoy OM, Yan Z, Gvasaliya S, Qiu Y, Ressouche E, Beauvois K, Raymond S, Ponomaryov AN, Zvyagin SA, Zheludev A. Magnetic structure and spin waves in the frustrated ferro-antiferromagnet $Pb_2VO(PO_4)_2$. Phys Rev B. 2019;99(18):184437.
[119] Yu XZ, Tokunaga Y, Kaneko Y, Zhang WZ, Kimoto K, Matsui Y, Taguchi Y, Tokura Y. Biskyrmion states and their current-driven motion in a layered manganite. Nat Commun. 2014;5:3198.
[120] Peng LC, Zhang Y, Wang WH, He M, Li LL, Ding B, Li JQ, Sun Y, Zhang XG, Cai JW, Wang SG, Wu GH. Real-space observation of nonvolatile zero-field biskyrmion lattice generation in MnNiGa magnet. Nano Lett. 2017;17(11):7075.
[121] Wang WH, Zhang Y, Xu GZ, Peng LC, Ding B, Wang Y, Hou ZP, Zhang XM, Li XY, Liu E, Wang SG, Cai JW, Wang FW, Li JQ, Hu FX, Wu GH, Shen BG, Zhang XX. A centrosymmetric hexagonal magnet with superstable biskyrmion magnetic nanodomains in a wide temperature range of 100–340 K. Adv Mater. 2016;28(32):6887.
[122] Peng LC, Zhang Y, He M, Ding B, Wang WH, Tian HF, Li JQ, Wang SG, Cai JW, Wu GH, Liu JP, Kramer MJ, Shen BG. Generation of high-density biskyrmions by electric current. npj Quantum Mater. 2017;2:30.
[123] Yu XZ, Tokunaga Y, Taguchi Y, Tokura Y. Variation of topology in magnetic bubbles in a colossal magnetoresistive manganite. Adv Mater. 2017;29(3):1603958.
[124] Yu XZ, Mostovoy M, Tokunaga Y, Zhang WZ, Kimoto K, Matsui Y, Kaneko Y, Nagaosa N, Tokura Y. Magnetic stripes and skyrmions with helicity reversals. Proc Natl Acad Sci USA. 2012;109(23):8856.
[125] Yuan S, Chen WJ, Liu JY, Liu Y, Wang B, Zheng Y. Torsion-induced vortex switching and skyrmion-like state in ferroelectric nanodisks. J Phys Condens Matter. 2018;30(46): 465304.
[126] Zhou HA, Liu JH, Wang ZD, Zhang QH, Xu T, Dong YQ, Zhao L, Je SG, Im MY, Xu K, Zhu J, Jiang WJ. Rare-earth permanent magnet $SmCo_5$ for chiral interfacial spin-orbitronics. Adv Funct Mater. 2021. https://doi.org/10.1002/adfm.202104426.
[127] Herbst JF, Croat JJ, Pinkerton FE. Relationships between crystal structure and magnetic properties in $Nd_2Fe_{14}B$. Phys Rev B. 1984;29:4176(R).
[128] Skomski R, Sellmyer. Intrinsic and extrinsic properties of advanced magnetic materials. In: Liu Y, Sellmyer DJ, Shindo D, editors. Handbook of advanced magnetic materials. Beijing: Tsinghua University Press; 2006. 3.
[129] Xiao Y, Morvan FJ, He AN, Wang MK, Luo HB, Jiao RB, Xia WX, Zhao GP, Liu JP. Spin-orientation transition induced magnetic skyrmion in $Nd_2Fe_{14}B$ magnet. Appl Phys Lett. 2020; 117:132402.
[130] Hou ZP, Li LW, Liu C, Gao XS, Ma ZP, Zhou GF, Peng Y, Yan M, Zhang XX, Liu JM. Emergence of room temperature stable skyrmionic bubbles in the rare earth based $REMn_2Ge_2$(RE = Ce, Pr, and Nd) magnets. Mater Today Phys. 2021;17:100341.
[131] Zhang XC, Zhao GP, Xia J, Yue M, Yuan XH, Xie LH. Micromagnetic simulation of Sm-Co/α-Fe/Sm-Co trilayers with various angles between easy axes and the film plane. Chin Phys B. 2014;23(9):097504.
[132] Zhao GP, Wang XL. Nucleation, pinning, and coercivity in magnetic nanosystems: an analytical micromagnetic approach. Phys Rev B. 2006;74:012409.
[133] Zhang W, Zhao GP, Yuan XH, Ye LN. 3D and 1D micromagnetic calculation for hard/soft bilayers with in-plane easy axes. J Magn Magn Mater. 2012;324(24):4231.
[134] Weng XJ, Zhao GP, Tang H, Shen LC, Xiao Y. Thickness-dependent coercivity mechanism and hysteresis loops in hard/soft magnets. Rare Met. 2020;39(1):22.
[135] Lai P, Zhao GP, Tang H, Ran N, Wu SQ, Xia J, Zhang X, Zhou Y. An improved racetrack structure for transporting a skyrmion. Sci Rep. 2017;7:45330.
[136] Juge R, Bairagi K, Rana KG, Vogel J, Sall M, Mailly D, Pham VT, Zhang Q, Sisodia N, Foerster M, Aballe L, Belmeguenai M, Roussigné Y, Auffret S, Buda-Prejbeanu LD, Gaudin G, Ravelosona D, Boulle O. Helium ions put magnetic skyrmions on the track. Nano Lett. 2021;21(7):2989.
[137] Ohara K, Zhang XC, Chen YL, Wei ZH, Ma YG, Xia J, Zhou Y, Liu XX. Confinement and protection of skyrmions by patterns of modified magnetic properties. Nano Lett. 2021;21(10): 4320.
[138] Feng YH, Xia J, Qiu L, Cai XR, Shen LC, Morvan FJ, Zhang XC, Zhou Y, Zhao GP. A skyrmion-based spin-torque nano-oscillator with enhanced edge. J Magn Magn Mater. 2019;491:165610.
[139] Shen LC, Xia J, Zhao GP, Ezawa M, Tretiakov OA, Liu XX, Zhou Y. Spin torque nano-oscillators based on antiferromagnetic skyrmion. Appl Phys Lett. 2019;114:042402.
[140] Shen LC, Xia J, Zhao GP, Zhang XC, Ezawa M, Tretiakov OA, Liu XX, Zhou Y. Dynamics of the antiferromagnetic skyrmion induced by a magnetic anisotropy gradient. Phys Rev B. 2018; 98:134448.
[141] Jungwirth T, Marti X, Wadley P, Wunderlich J. Antiferromagnetic spintronics. Nat Nanotech. 2016;11:231.
[142] Liang X, Zhao GP, Shen LC, Xia J, Zhao L, Zhang XC, Zhou Y. Dynamics of an antiferromagnetic skyrmion in a racetrack with a defect. Phys Rev B. 2019;100:144439.
[143] Morvan FJ, Luo HB, Yang HX, Zhang X, Zhou Y, Zhao GP, Xia WX, Liu JP. An achiral ferromagnetic/chiral antiferromagnetic bilayer system leading to controllable size and density of skyrmions. Sci Rep. 2019;9:2970.
[144] Caretta L, Mann M, Büttner F, Ueda K, Pfau B, Günther CM, Hessing P, Churikova A, Klose C, Schneider M, Engel D, Marcus C, Bono D. Bagschik, Eisebitt, Bearch GSD. Fast current-driven domain walls and small skyrmions in a compensated ferrimagnet. Nat Nanotech. 2018;13(12):1154.
[145] Woo S, Song KM, Zhao XC, Ezawa M, Zhou Y, Liu XX, Weigand M, Finizio S, Raabe J, Park MC, Lee KY, Choi JW, Min BC, Koo HC, Chang J. Deterministic creation and deletion of a single magneic skyrmion observed by direct time-resolved X-ray microscopy. Nat Electron. 2018;1(5):288.
[146] Chen K, Lott D, Philippi-kobs A, Weigan M, Luo C, Radu F. Observation of compact ferrimagnetic skyrmions in $DyCo_3$ film. Nanoscale. 2020;12(35):18137.
[147] Mandru AO, Yıldırım O, Tomasello R, Heistrcher P, Penedo M, Giordano A, Suess D, Finocchio G, Hug HJ. Coexistence of distinct skyrmion phases observed in hybrid ferromagnetic/ferrimangetic multilayers. Nat Commun. 2020;11:6365.
[148] Liang X, Xia J, Zhang XC, Ezawa M, Tretiakov OA, Liu XX, Qiu L, Zhao GP, Zhou Y. Antiferromagnetic skyrmion-based logic gates controlled by electric currents and fields. Appl Phys Lett. 2021;119:062403.
[149] Liang X, Zhang XC, Xia J, Ezawa M, Zhao YL, Zhao GP, Zhou Y. A spiking neuron constructed by the skyrmion-based

spin torque nano-oscillator. Appl Phys Lett. 2020;116(12):122402.
[150] Zhao L, Liang X, Xia J, Zhao GP, Zhou Y. A ferromagnetic skyrmion-based diode with voltage-controlled potential barrier. Nanoscale. 2020;12(17):9507.
[151] Zhang XC, Zhou Y, Ezawa M, Zhao GP, Zhao WS. Magnetic skyrmion transistor: skyrmion motion in a voltage gated nanotrack. Sci Rep. 2015;5:11369.
[152] Song KM, Jeong JS, Pan B, Zhang XC, Xia J, Cha S, Park TE, Kim K, Finizio S, Raabe J, Chang J, Zhou Y, Zhao WS, Kang W, Ju H, Woo S. Skyrmion-based artificial synapses for neuromorphic computing. Nat Electron. 2020;3(3):148.
[153] Yan H, Feng ZX, Shang SL, Wang XN, Hu ZX, Wang JH, Zhu ZW, Wang H, Chen ZH, Hua H, Lu WK, Wang JM, Qin PX, Guo HX, Zhou XR, Leng ZGG, Liu ZK, Jiang CB, Coey M, Liu ZQ. A piezoelectric, strain-controlled antiferromagnetic memory insensitive to magnetic fields. Nat Nanotech. 2019;14(2):131.
[154] Liu ZQ, Feng ZX, Yan H, Wang XN, Zhou XR, Qin PX, Guo HX, Yu RH, Jing CB. Antiferromagnetic piezospintronics. Adv Electron Mater. 2019;5(7):1900176.

Guo-Ping Zhao received B.S. and Ph.D. degrees of Physics in 1990 and 2003, respectively, from University of Science and Technology of China and National University of Singapore (NUS). He worked in NUS from 2000 to 2004. Since 2004, he has been a professor and distinguished professor in Sichuan Normal University (SICNU). Prof. Zhao is the founder and director of the Magnetic Materials Lab, SICNU. He is the author or the coauthor of more than 100 SCI papers published in international journals and referred conferences, including more than 20 on ferromagnetic and antiferromagnetic skyrmion dynamics. Currently, Prof. Zhao acts as a managing guest editor for the special issue "Topological Spin Texture" to be published in Journal of Magnetism and Magnetic Materials.